Journal of Alloys and Compounds 504S (2010) S180–S185

Contents lists available at ScienceDirect

Journal of Alloys and Compounds

journal homepage: www.elsevier.com/locate/jallcom

The oxidation behavior of a $Ti_{50}Cu_{28}Ni_{15}Sn_7$ bulk metallic glass at 400–500 °C

W. Kai*, P.C. Kao, W.S. Chen, C.L. Lin, Z.H. Xiao, C.F. Hsu, P.Y. Lee

Institute of Materials Engineering, National Taiwan Ocean University, Keelung 20224, Taiwan, ROC

ARTICLE INFO

Article history:
Received 3 July 2009
Received in revised form 16 April 2010
Accepted 24 April 2010
Available online 15 May 2010

Keywords:
$Ti_{50}Cu_{28}Ni_{15}Sn_7$ bulk metallic glass
Oxidation
TiO_2
CuO

ABSTRACT

The oxidation behavior of a $Ti_{50}Cu_{28}Ni_{15}Sn_7$ bulk metallic glass (TC4-BMG) was studied over the temperature range of 400–500 °C in dry air. The oxidation kinetics generally followed the parabolic-rate law, and the oxidation rates increased with increasing temperature. The scales formed on the TC4-BMG consisted mostly of TiO_2 (rutile structure) intermixed with small amounts of CuO particles. It was found that the scaling rate of the amorphous alloy was slightly faster than that of the crystalline counterpart. The amorphous substrate transferred into the three crystalline phases of Ti_3Sn, Ti_3Cu_4, and Ti(Ni,Cu) during the oxidation at 400–500 °C, indicating the occurrence of phase transformation.

1. Introduction

Titanium-based amorphous alloys, such as Ti–Be, Ti–Ni, or Ti–Be–Zr systems, have been developed since the early 1980s because of their excellent mechanical stability and good aqueous-corrosion resistance with respect to commercial Ti-based alloys [1–3]. Particularly, they are of interest for good chemical stability to be used for artificial bones in human beings.

In 1998, Inoue et al. reported that an additional 5%Sn (in at.%) greatly improved the supercooled temperature (ΔT_x) and the glass forming ability (GFA) of the Ti–Cu–Ni-based bulk metallic glasses (BMGs) produced by the commercial Cu-mold casting technique [4–7]. The maximum diameter of the 5%Sn-containing BMG rod was around 6 mm.

Most recently, a similar quaternary BMG with the nominal composition of Ti–28Cu–15Ni–7Sn (TC4-BMG; in at.%) was synthesized through mechanical-alloying plus vacuum hot-pressing in our laboratory [8]. It appeared that a 10-mm diameter and 2-mm thickness of this amorphous disc was successfully fabricated. In addition, one of our published studies showed that the TC4-BMG exhibited a high Vickers hardness value of 6.85 GPa, and a compressive fracture strength of 1.69 GPa with nearly zero plastic strain [8]. In spite of several studies on the mechanical properties of the Ti-based BMGs, their oxidation behavior has not yet been investigated. Therefore, it is of great interest to study the oxidation behavior of the TC4-BMG, and in particular to realize the role of alloying elements on the oxidation kinetics.

2. Experimental

The TC4-BMG discs were prepared by a mechanical-alloying plus vacuum hot-pressing technique described previously [8]. The density data of the amorphous alloy measured using Archimede's method [9] showed that an average value of 97.6% theoretical density was achieved. The BMG samples were sheared into a quarter-disc shape (about 4.5 mm × 4.5 mm × 2 mm), ground and polished to 1-μm diamond paste, cleaned with acetone and methanol, and immediately dried before the tests. For comparative purposes, a few BMG samples were further vacuum annealed at 600 °C for 1 h to obtain the crystalline counterpart samples (XTC4). In addition, the pure Ti samples (commercial grade, >99.9% pure) were also cut into a rectangle shape (10 mm × 5 mm × 2 mm), and then, both pure Ti and XTC4 samples were subsequently oxidized at the same condition as the TC4-BMG.

The thermal stability of the TC4-BMG was analyzed by differential scanning calorimetry (DSC) at various heating rates. The oxidation tests were performed by means of a horizontal tube-furnace in dry air (>99.99% vol.% pure). The net flow rate of dry air was kept constant at 40 cm^3/min throughout each test, and the heating and cooling rates of the furnace were set at 10 °C/min. The scale thickness was measured by the metallurgical analyses using scanning electron microscopy (SEM) under backscattered electron-image (BEI) mode. At least 20 values of the scale thickness were taken at each temperature and individual exposure time under the standard procedure of ASTM-G54 [10]. The oxidation kinetics was determined using the double log-plots of the scale thickness vs. time, and then, the scaling rate constants of the samples were calculated. The characterization of the alloys and scales was performed using X-ray diffraction (XRD), SEM equipped with energy-dispersive spectrometry (EDS), electron probe microanalyzer (EPMA) equipped with wavelength-dispersive spectrometry (WDS), and transmission electron microscopy (TEM) equipped with EDS and selected-area diffraction (SAD).

3. Results and discussion

3.1. Substrate analyses

Although not shown here, XRD analyses of the TC4-BMG only contained a wide-broadening peak at $2\theta = 42.05°$, indicative of the amorphous nature for the substrate. On the other hand, the XTC4

* Corresponding author: Tel.: +886 2 24622192x6403; fax: +886 2 24625324.
E-mail address: wkai@mail.ntou.edu.tw (W. Kai).

0925-8388/$ – see front matter.
doi:10.1016/j.jallcom.2010.04.128

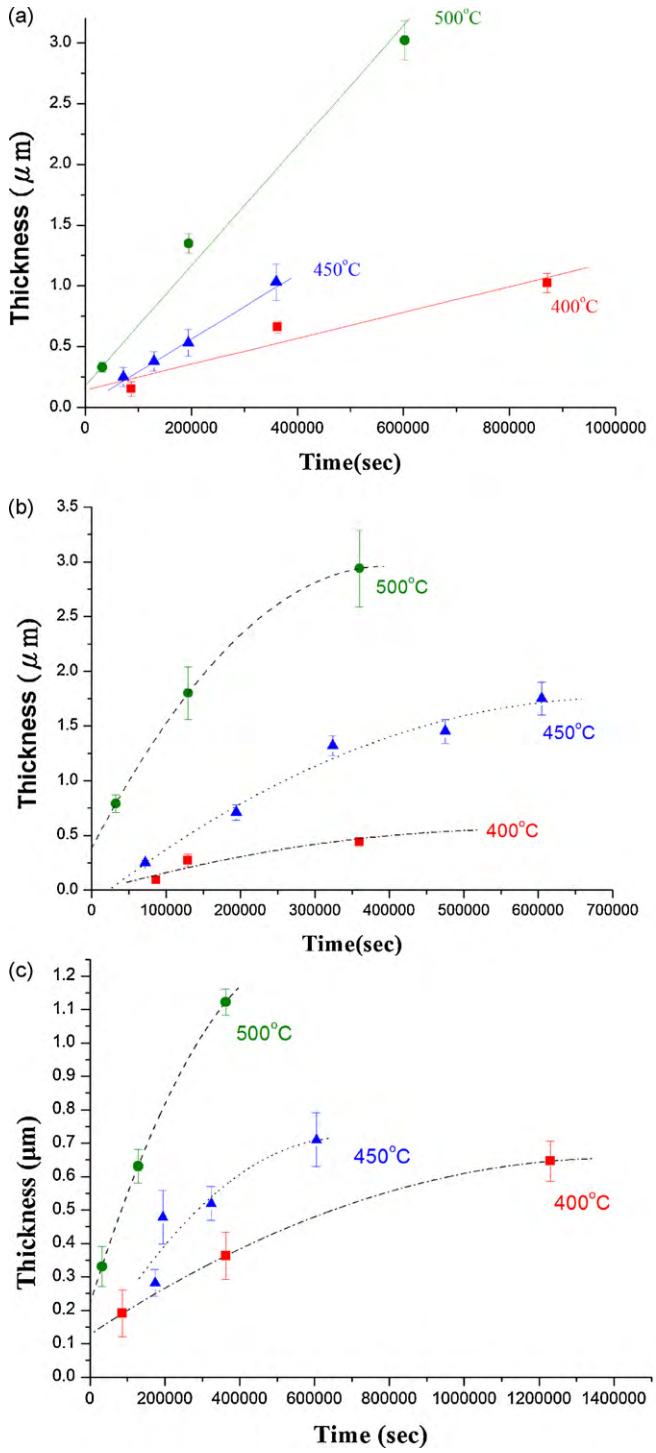

Fig. 1. Linear plots of the oxidation kinetics at 400–500 °C (a) pure Ti, (b) TC4-BMG, and (c) XTC4.

alloy revealed a triplex structure, consisting of Ti_3Cu_4, Ti_3Sn, and Ti(Ni,Cu). The grain size of the three crystalline phases was estimated by the Scherrer formula [11], as given by the equation of $d = 0.9\lambda/B\cos\theta_B$, where d, λ, B, and θ_B are the calculated grain size, wavelength of X-ray, full width at half maximum intensity (in radians), and diffraction angle at the peak position, respectively. The results of the average grain size of these phases from the possible diffraction planes are around 24.6 ± 3.6, 26.6 ± 6.7, and 20.9 ± 1.0 nm for Ti_3Cu_4, Ti_3Sn, and Ti(Ni,Cu), respectively. In addition, the DSC curves of the TC4-BMG (also not shown here) revealed

Table 1
The scaling rate constants of Ti-based alloys ($\mu m^2/s$).

	400 °C	450 °C	500 °C
TC4-BMG	4.27×10^{-7}	2.50×10^{-6}	1.60×10^{-5}
XTC4	3.59×10^{-7}	8.42×10^{-7}	3.50×10^{-6}

that the glass transition temperature (T_g) at heating rates of 10, 20, and 40 °C/min was about 414.7, 435.6, and 445.3 °C, respectively, while the crystalline temperature (T_x) at the same heating rates was about 454.5, 476.1, and 484.5 °C, respectively. Thus, the supercooled temperature (ΔT_x) was about 39.8 °C, and the oxida-

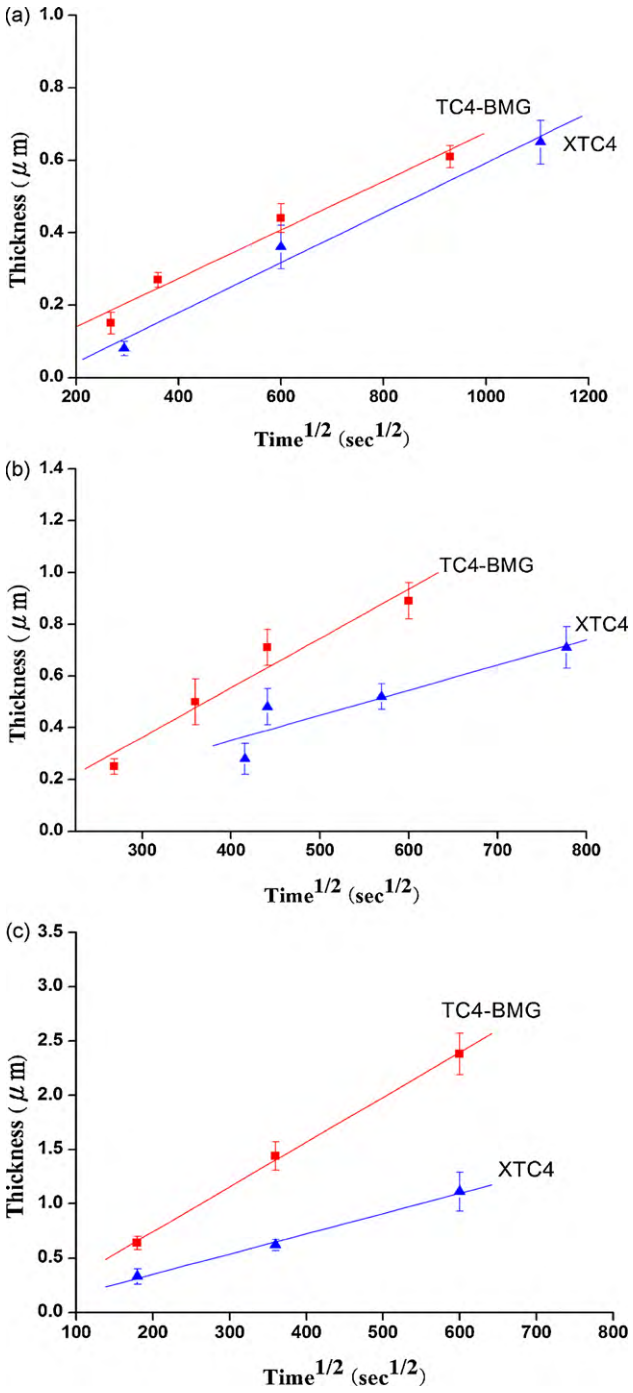

Fig. 2. Parabolic plots of the oxidation kinetics of TC4-BMG and XTC4 alloys at (a) 400 °C, (b) 450 °C, and (c) 500 °C.

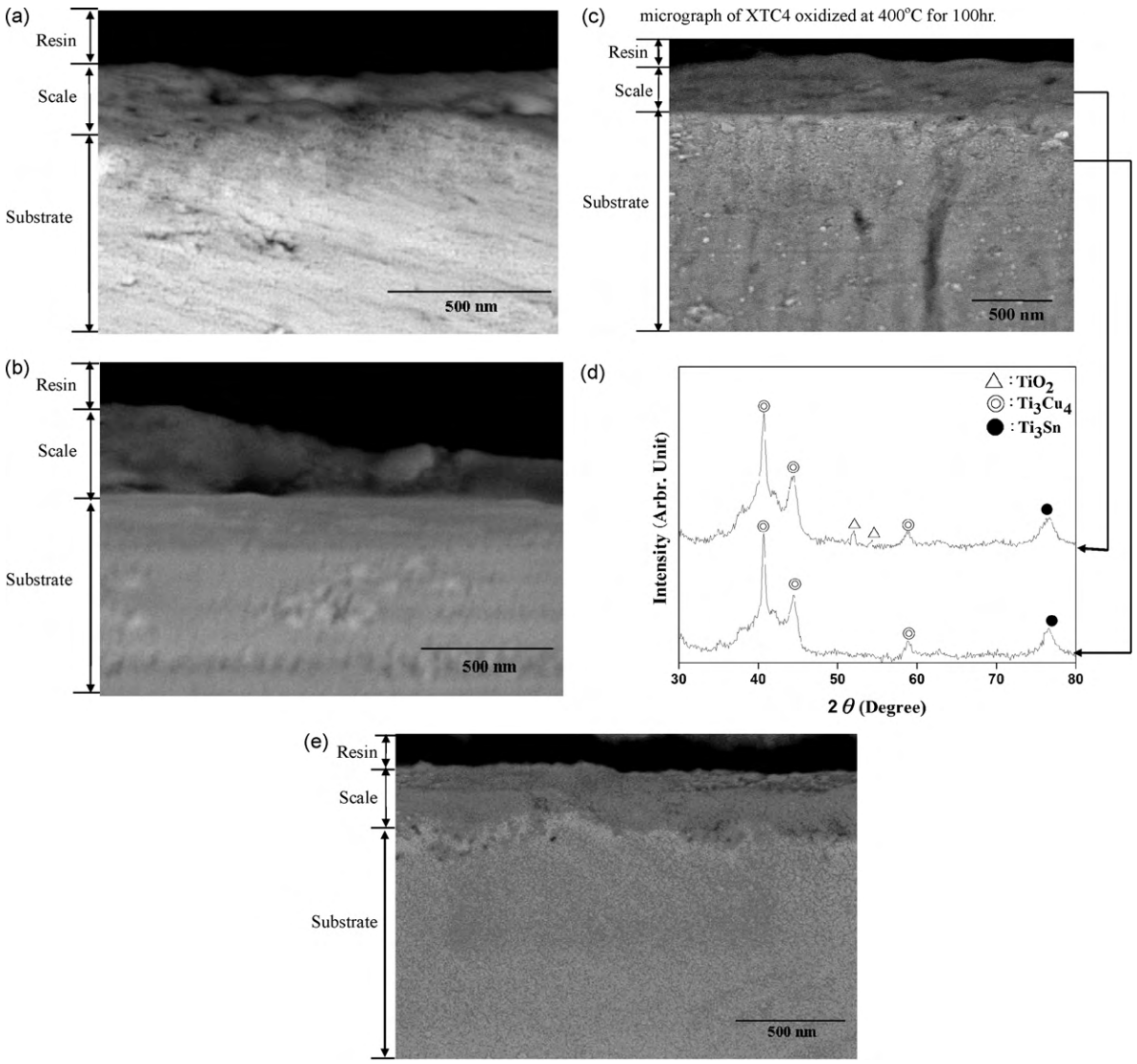

Fig. 3. Cross-sectional BEI micrographs of TC4-BMG oxidized at 400 °C for (a) 24 h, (b) 36 h, (c) 100 h, (d) corresponding XRD for (c), and (e) cross-sectional BEI micrograph of XTC4 oxidized at 400 °C for 100 h.

tion tests were set over the temperature range of 400–500 °C to cover from the amorphous to crystalline states.

3.2. Oxidation kinetics

The linear plots of the oxidation kinetics of TC4-BMG, XTC4, and pure Ti over the temperature range of 400–500 °C are shown in Fig. 1. According to the scaling rate theory [12], the oxidation kinetics can be described as an equation between the scale thickness (X) and the exposure time (t)

$$X = Kt^n + C \quad (1)$$

where n could be determined by the slope of the double log-plot of the scale thickness vs. time, and K and C are the rate constant and integration constant, respectively. As shown in Fig. 1, the linear fitting is obtained for pure Ti (having an n value of ~1.0) although the data scattering is slightly larger at 400 °C. This observation indicated that the oxidation kinetics of pure Ti followed the linear-rate law, and the interface reaction on top of the sample surface prevailed in the thermal-activated process. On the other hand, the curve fitting was obtained for both TC4-BMG and XTC4 alloys (having an n value of ~0.5), implying that the parabolic-rate law was obeyed, and diffusion was the rate-determining step during oxidation. Since the oxidation kinetics of pure Ti differed from those of the two alloys, the follow sections only discuss the scaling rate constants and scale constitution of the two alloys.

The parabolic plots of the oxidation kinetics of the alloys, in terms of the scale thickness vs. square-root of time, over the temperature range of 400–500 °C in dry air are shown Fig. 2. The scaling rate constants (k_s values) calculated by the square of the slope in the figure were tabulated in Table 1. Clearly, the k_s values of the two alloys increased steadily with increasing temperature. In addition, it should be pointed out that the k_s values of the TC4-BMG are slightly higher than those of its crystalline counterpart, indicative of a poor oxidation resistance for the amorphous alloy. The discrepancy of the k_s values for the amorphous and crystalline alloys may be due primarily to the formation of various scales, which deserves further studies in the following section.

3.3. Scale constitution and phases

Typical cross-sectional BEI micrographs of the TC4-BMG oxidized at 400 °C for various durations of time are shown in Fig. 3a–c, revealing a thin-scale layer which has good adherence with the

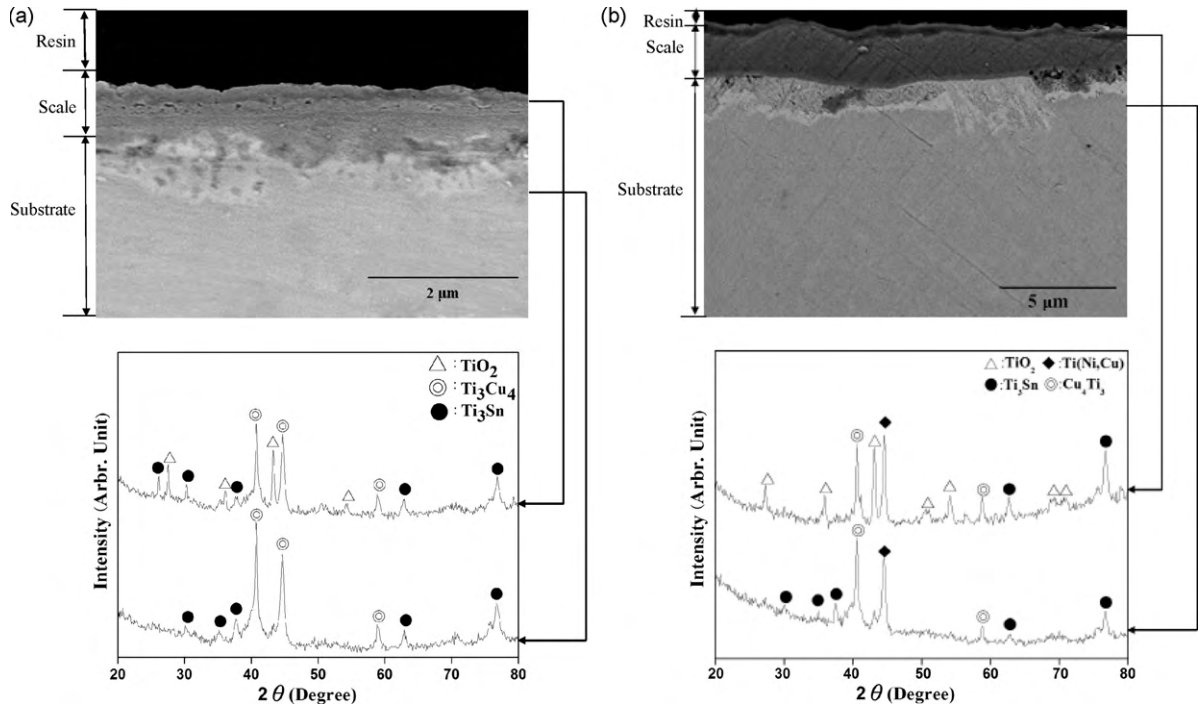

Fig. 4. Cross-sectional BEI micrographs and corresponding XRD of the TC4-BMG oxidized for 100 h at (a) 450 °C and (b) 500 °C.

substrate. The scale thickness gradually increased with increasing duration of time, being around 0.15 ± 0.03, 0.27 ± 0.06, and 0.44 ± 0.04 μm after a 20-, 36-, and 100-h exposure, respectively. The XRD spectra (Fig. 3d) revealed that the scales consisted of a mixture of titanium oxide (TiO_2) and uncorroded intermetallics mostly of Ti_3Cu_4 and minor amount of Ti_3Sn and Ti(Ni,Cu). The presence of these crystalline phases could be due to the thin-scale nature, which allows the X-ray source penetrated down to the substrate. Besides, it is also interesting to note that some dark-image regions were observed inside the scale; yet, both EDS and WDS failed to obtain the exact composition. Nevertheless, the formation of the three crystalline phases further indicated that the phase transformation of the glassy substrate was taken place although the oxidation temperature is much lower than T_g (414.7 °C). In addition, a BEI micrograph of the XTC4 alloy oxidized at the same temperature for 100 h is also shown in Fig. 3e for comparative purposes. Note that the scale thickness of XTC4 is around 0.36 ± 0.04 μm, which is thinner than that of TC4-BMG under the same exposure time. This observation is in good agreement with the kinetics measurement, as described above.

In addition, BEI micrographs and corresponding XRD spectra of the TC4-BMG oxidized at 450 and 500 °C for 100 h are shown in Fig. 4. The XRD results at both temperatures were similar to those at 400 °C, except that the amounts of TiO_2 and Ti_3Sn were much abundant. In addition, the thickness of the scales at 450 and 500 °C is about 0.89 ± 0.07, and 2.38 ± 0.19 μm, respectively. Apparently, their thickness at both temperatures is much thicker than that at 400 °C under the same exposure time. This observation is also in good agreement with the kinetics measurement, in which the higher the temperature is the fast the transport of anions and the higher the scaling rates. Another interesting aspect should be pointed out that a thin, bright zone beneath the scales was present at both temperatures, and its thickness also increased with increasing temperature, being about 0.4 (450 °C) to 1.2 (500 °C) μm. EDS analyses gave the average composition of Ti (33.7%), Cu (28.2%), Ni (15.0%), Sn (13.0%), and O (10.1%) in this zone at 500 °C, which indicated that both Cu and Ni concentrations remained nearly unchanged, while Ti was depleted but Sn was enriched with respect to the initial composition of TC4-BMG. Most likely, the observed bright image under a SEM/BEI mode indicates that the relative amount of Ti_3Sn in this zone is much abundant because its average atomic-weight (65.6) is higher than that of both Cu_4Ti_3 (56.8) and Ti(Ni,Cu) (56.7). Thus, the higher the oxidation temperature (500 °C in this study), the more the amount of Ti_3Sn formed beneath the scales, which in turn results in the thicker bright zone, as indicated above.

Besides, according to the literature [13,14], TiO_2 was the only stable phase present in the oxidation of pure Ti, and its predominant defects were double ionized oxygen vacancies [$V_o^{\bullet\bullet}$]. According to the Gibbs free energies of formation of the possible oxides, TiO_2 (−811.8 kJ/mol of O_2 at 450 °C) is the most stable oxide and it should therefore be expected to form for both TC4-BMG and its crystalline counterpart. As also mentioned previously [15], titanium has high affinity for oxygen, and the oxygen solubility in its α phase is around 30.0%. Thus, one would expect that only TiO_2 would develop and the scaling rates should be nearly identical for both BMG and crystalline alloys because the activity of Ti is much higher than that of other alloying elements. However, the kinetics results (Table 1) revealed the fact that the scaling rates of the glassy alloy is indeed much faster than those crystalline counterpart. Therefore, it is necessary to further clarify the exact scale constitution and phases through TEM analyses. Typical TEM cross-sectional scales formed after oxidized at 450 °C for 100 h for both TC4-BMG and XTC4 alloys were prepared; the results together with the corresponding SAD patterns are shown in Fig. 5. It is clear that an exclusive layer of TiO_2 with various crystalline orientations is always present for the XTC4 alloy, while small amounts of CuO particles embedded into the TiO_2 layer were detected for the TC4-BMG. The observation of CuO in the scales of TC4-BMG, however, disagreed with the XRD results, as described above. Very likely, the amounts of CuO in the scales are too low to be detected or beyond the X-ray detection limits. Thus, TEM analyses confirmed that the CuO phase indeed formed in the scales, and its formation certainly deserves further discus-

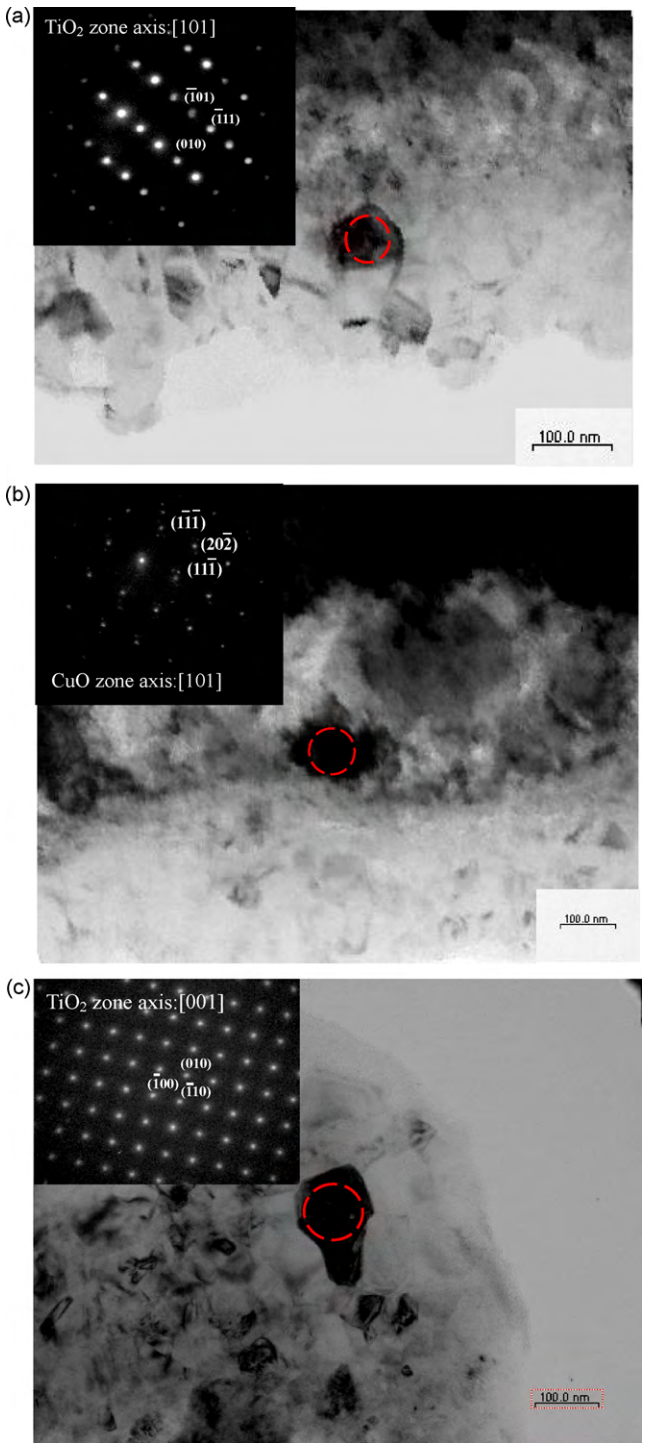

Fig. 5. TEM micrographs and SAD patterns oxidized at 450 °C for 100 h at various regions of the scales of (a) and (b) for TC4-BMG, and (c) for XTC4 alloy.

sion for the two possible reasons of faster scaling rate constants of TC4-BMG.

First of all, an amorphous alloy can be considered as a metastable phase in equilibrium with its atomic packing of a short- to medium-range order, which creates many sites in its lattice structure, which resulted in the excess free volume, as similar to that reported previously [16]. It is very likely that the created free volume acts as a fast diffusion path for inward oxygen-diffusion, which in turn increased the oxygen penetration through the substrate, thereby accelerating the scaling rates for the amorphous alloy. Thus, it is expected that TC4-BMG undergoes a fast gas–metal reaction, leading to its higher oxidation rates with respect to those of its crystalline counterpart.

Secondly, as mentioned above, the amorphous substrate is not fully compact (97.6% dense), so that a small amount of porosity expected to exist inside the TC4 alloy. It seemed that the porosity may play an important role in enhancing inward oxygen-diffusion, which in turn may result in an increase of the oxygen activity in the local regions around the TiO_2/substrate boundary, thereby favoring the formation of other oxides. In other words, when the TiO_2 phase formed, it would consume certain amounts of Ti in the bright zone of the substrate, which in turn cause a possibility of forming CuO/Cu_2O, NiO, or SnO_2 at the later stage of oxidation. Although the Gibbs free energies of formation (in the same unit of kJ/mol of O_2 at 450 °C) of NiO (−346.1) and SnO_2 (−430.9) are much more negative than those of CuO (−180.1) and Cu_2O (−231.5), copper would have a much higher activity than Ni and Sn, which gave it a better probability to react with oxygen to form copper oxides that intermixed with TiO_2 in the scales of TC4-BMG. According to another published work in our laboratory [17], the non-stoichiometry value (y) for TiO_{2-y} was reported to be about 0.01 at 900 °C, and it decreased with decreased temperature, while that of CuO remained unclear. It may be induced that the formation of CuO could reduce the oxidation rate of TC4-BMG if its defect concentration is lower than that of TiO_2. However, the results came out in an opposite direction, so that it is most likely that the defect concentration of CuO may be slightly higher than that of TiO_2. Thus, the higher the oxygen

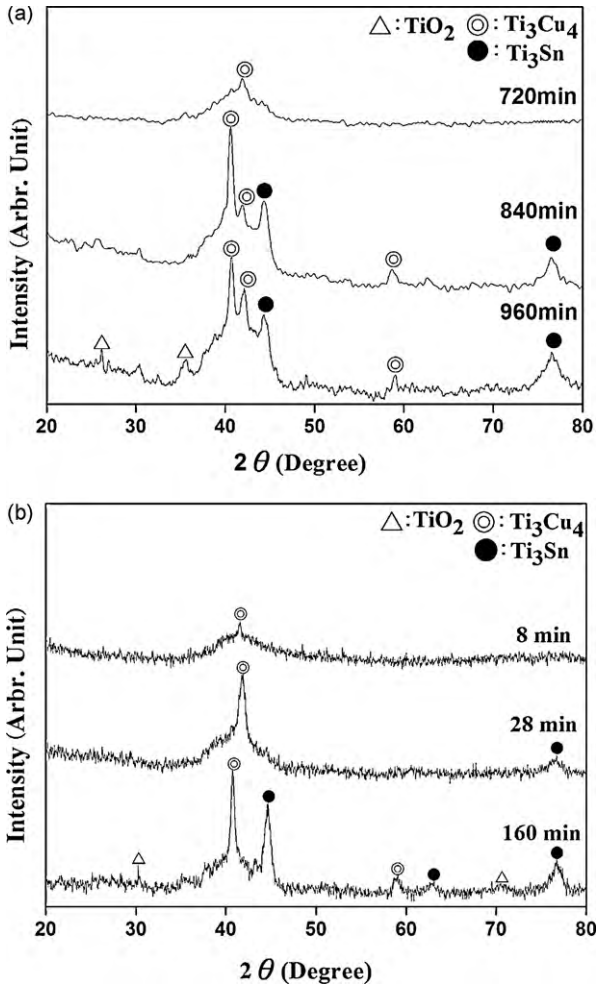

Fig. 6. XRD analyses of the scales formed on the TC4-BMG for various durations of time at (a) 400 °C and (b) 500 °C.

vacancies presents in the TC4-BMG, the faster of inward oxygen-diffusion in the scales, thereby leading to the faster oxidation rates, as compared to those of XTC4.

3.4. Short-term oxidation

To understand the relationship between the oxidation of crystallization of the TC4-BMG, two short-term oxidation tests were carried out. Typical XRD spectra of the TC4-BMG after the oxidation at various durations of time at 400 and 500 °C are shown in Fig. 6. Obviously, a Ti_3Cu_4 phase exclusively formed on the amorphous substrate after an initial oxidation at 400 °C for 720 min, and additional Ti_3Sn and Ti(Ni,Cu) phases was also detected after an 840-min exposure at the same temperature. This indicated that the TC4-BMG started to form the two intermetallics before its oxidation was occurred. After a prolong exposure of 960 min, a few amounts of TiO_2 were observed. In addition, the short-term oxidation at 500 °C followed a similar trend at 400 °C except that duration of time for the amorphous to crystalline transformation is much shorter, being about 8 min for the first growth of Ti_3Cu_4, 28 min for the second growth of Ti_3Sn, and 160 min for the formation of Ti(Ni,Cu) and TiO_2. Thus, the whole phase transformation of the TC4-BMG is governed first by the crystallization of Ti_3Cu_4, followed by the crystallization of Ti_3Sn and Ti(Ni,Cu), and then, the formation of TiO_2 and CuO (not possible to be detected by XRD as mentioned above) at the later stage of oxidation.

4. Conclusions

The oxidation behavior of the quaternary $Ti_{50}Cu_{28}Ni_{15}Sn_7$ BMG (TC4-BMG) and crystalline alloys over the temperature range of 400–500 °C in dry air was characterized. Several conclusions were drawn as follows:

1. Oxidation kinetics of the TC4-BMG and its crystalline counterpart follows the parabolic-rate law over the temperature range of interest.
2. The scaling rate constants of the TC4-BMG are slightly higher than those of the crystalline counterpart, indicative of a poor oxidation resistance for the amorphous alloy.
3. The scales formed on the BMG alloy consisted of TiO_2 intermixed with minor amounts of CuO, while an exclusive TiO_2 layer formed on the crystalline counterpart.
4. The formation of CuO increased the concentration of oxygen vacancies in the TiO_2 lattice, which enhanced inward diffusion of oxygen, thereby leading to the faster oxidation rates of the TC4-BMG, as compared to those of the crystalline counterpart.

Acknowledgements

The authors are thankful for the partly financial support by the National Science Council of Republic of China under the Grant Nos. NSC-96-2218-E-110-001 and NSC-97-2221-E-019-004 is greatly appreciated. Special gratitude is due to Dr. R.T. Huang of our institute and Mr. C.T. Wu, the Department of System Engineering and Science, National Tsing Hua University (Hsin-Chu, Taiwan), for their great assistance on technical supports of TEM. The SEM equipment support from the National Taiwan Ocean University under Grant No. NTOU-AP94-04-03-01-01 is also acknowledged.

References

[1] L.E. Tanner, R. Ray, Scripta Mater. 11 (1977) 783.
[2] D.E. Polk, A. Calka, B.C. Giessen, Acta Mater. 26 (1978) 1097.
[3] L.E. Tanner, R. Ray, Acta Mater. 27 (1979) 1727.
[4] T. Zhang, A. Inoue, T. Masumoto, Mater. Sci. Eng. A 181–182 (1994) 1423.
[5] T. Zhang, A. Inoue, Mater. Trans. JIM 39 (1998) 1001.
[6] A. Inoue, Mater. Sci. Forum 312–314 (1999) 307.
[7] A. Inoue, Acta Mater. 48 (2000) 279.
[8] C.-F. Hsu, H.-M. Lin, P.-Y. Lee, Adv. Eng. Mater. 10 (2008) 1053.
[9] A.R. Robinson, S.R. Elliott, J. Bone Joint Surg. Am. 39 (1957) 167.
[10] ASTM Standard G54-84, ASTM, USA, 1991, p. 199.
[11] D.B. Cullity, S.R. Stock, Elements of X-ray Diffraction, 3rd ed., Prentice Hall, New Jersey, 2001.
[12] N. Birks, G.H. Meier, Introduction to High Temperature Oxidation of Metals, Edward Arnold, London, 1983.
[13] R.N. Blumenthal, D.H. Whitmore, J. Electrochem. Soc. 110 (1963) 92.
[14] P. Kofstad, High Temperature Corrosion, Elsevier Applied Science, London and New York, 1988.
[15] P. Kofstad, Nonstoichiometry, Diffusion and Electrical Conductivity in Binary Metal Oxides, Robert E. Krieger Publishing Company, Florida, 1983.
[16] W. Kai, H.H. Hsieh, T.H. Ho, R.T. Huang, Y.L. Lin, Oxid. Met. 68 (2007) 177.
[17] H.H. Hsieh, W. Kai, W.L. Jang, R.T. Huang, P.Y. Lee, W.H. Wang, Oxid. Met. 67 (2007) 179.